

Entanglement and quantal coherence: a study of two limiting cases of rapid system–bath interactions

Nicole F. Bell¹, R. F. Sawyer² and Raymond R. Volkas¹

¹ *School of Physics, Research Centre for High Energy Physics*

The University of Melbourne, Victoria 3010 Australia

² *Department of Physics, University of California at Santa Barbara*

Santa Barbara, California 93106

(n.bell@physics.unimelb.edu.au, sawyer@vulcan.physics.ucsb.edu,

r.volkas@physics.unimelb.edu.au)

Pacs 3.65w, 3.67a, 5.40a

We consider the dynamics of a system coupled to a thermal bath, going beyond the standard two-level system through the addition of an energy excitation degree of freedom. Further extensions are to systems containing many fermions, with the master equations modified to take Fermi-Dirac statistics into account, and to potentials with a time-dependent bias that induce resonant avoided crossing transitions. The limit $Q \rightarrow \infty$, where the interaction rate with the bath is much greater than all free oscillation rates for the system, is interrogated. Two behaviors are possible: freezing (quantum Zeno effect) or synchronization (motional narrowing). We clarify the conditions that give rise to each possibility, making an explicit connection with quantum measurement theory. We compare the evolution of quantal coherence for the two cases as a function of Q , noting that full coherence is restored as $Q \rightarrow \infty$. Using an extended master equation, the effect of system-bath interactions on entanglement in bipartite system states is computed. In particular, we show that the synchronization case sees bipartite system entanglement fully preserved in the large Q limit.

I. INTRODUCTION

The dynamics of a quantum system coupled to a thermal bath is of great interest in many branches of physics [1]. This topic is of practical importance because no system apart from the universe as a whole is actually isolated. The contemporary focus on quantum computation [2] has been providing added impetus to these studies, as has the need to understand collision-affected neutrino oscillation dynamics in astrophysical and cosmological settings [3]. From a fundamental perspective, the effect of system-bath interactions on quantal coherence in the system bears on the measurement problem and on the emergence of classical behavior out of an underlying quantum dynamics [4].

In this paper we will revisit two closely related phenomena that arise in the limit of very rapid system-bath interactions: freezing (or quantum Zeno effect) and motional narrowing (or synchronization). Our intentions are twofold: (i) To present a unified perspective on these effects that emphasizes their connection with each other, and their connections to general quantal coherence and measurement questions. (ii) To extend the analysis to incorporate Fermi-Dirac statistics, a potentials with time dependent bias, and 2-particle entangled states. For definiteness we will focus on a double-well system, which turns out to be a versatile container for exemplifying and coordinating a number of phenomena. However almost all of our considerations can be carried over to other arenas, e. g. spin systems.

A. Freezing or Zeno

What we call freezing in this paper, the drastic slowing of a process through environmental interactions, can be discussed in a number of ways. If we start with an oscillator of some kind, and crank up a damping parameter to the point that the oscillator hardly budges in any reasonable amount of time, we might call the system overdamped. If we start with a decaying system on which we make very rapid measurements to see whether the original state is still there and find that the system has hardly evolved, we call it the quantum Zeno

effect (QZE) [5]. Except for the fact that something has been slowed, two behaviors that are described so differently appear to have little in common. But when the “over-damped” behavior in the oscillator comes from interactions with a quantum thermal bath, and the “observation” in the QZE is replaced by interactions of the system with such a bath as well, then we find that the two terminologies can describe the same essential physics. If we particularize the “oscillator” in the above to the case of a particle in a symmetrical double-well, then it turns out that we must require the bath interaction to distinguish left from right in order for freezing to occur; hereafter we shall refer to such a bath as “side-sensing”. Correspondingly, for the particle-decay prototype of the QZE, in order to simulate rapid measurements the bath must sense the presence or absence of the initial particle. For the widely discussed two-state systems, the freezing phenomenon is essentially the same whether they are double-well systems originating in a condensed matter context [1], molecules [6] [7], nuclear spins, squids [8], or neutrinos in the early universe [9].

In practical circumstances we shall want to know the answer to quantitative questions such as how frozen a system becomes as a result of bath interactions, the answers to which can be roughly expressed in terms of ratios of the different time scales in the problem. We also want to know how the slowing or freezing behavior is correlated to other calculable phenomena in the system.

B. “Synchronization in a linear system” or “motional narrowing”

These two effects seem to be identical at the formal level. They carry different names as a result of arising in very different physical contexts. Synchronization is a natural partner to the slowing or freezing phenomena for the case in which the bath does *not* distinguish which of the two states the two-state system is in. We shall describe such a coupling as “side-blind”. For a pure two state system, this describes an interaction that does nothing at all of note. But in our example of an electron in a symmetrical double well we may wish to place the system in a bath that can excite or deexcite the states that are higher

lying than the first two (i.e. higher lying than the nearly degenerate symmetrical and anti-symmetrical combinations of the single-well ground states). We shall refer to the inclusion of these states as the introduction of a “vertical” coordinate, using “horizontal” to denote the left and right coordinate. The oscillation rates are different for the higher-lying states, so that the density matrix for a particle that is, say, initially on one side of the well no longer oscillates sinusoidally between the two states. But in the limit of large “side-blind” coupling to the bath the simple sinusoidal behavior is restored, as though the different frequencies had been made the same, and the oscillations of the different vertical components synchronized. Similar behavior in a neutrino-based example has been reported in ref. [10]. “Motional narrowing” has been used to describe analogous behavior in an NMR system [11]. Qualitatively, motion narrowing occurs when the system is made to change state so rapidly that it is only able to respond to an average Hamiltonian. That is, the “horizontal” evolution is governed by parameters which are averaged over the “vertical” states.

In this paper we review the basic analysis required to establish the above assertions, including the derivation of a master equation, all in the double-well context, and we provide some plots of typical behavior of the solutions. Then we investigate a number of new topics related to the limits mentioned above:

1. Several fermions in the well

This entails writing a modified master equation to take into account Fermi statistics. The solutions, in the limit of large “side-blind” noise, have a counterintuitive property: an assemblage of several particles can move sinusoidally from one side to the other, giving the appearance of being in the same state.

2. Systems with four horizontal states

This is like the familiar case of two spin degrees of freedom; in our well realizations we utilize two independent particles in the well, each particle with the same structure of vertical

levels. We can now study entanglement of the horizontal states. In the presence of moderate “side-blind” noise we find rapid destruction of entanglement, while in the “synchronizing” limit of large “side-blind” noise we have, in contrast, perfect preservation of entanglement. The latter may find application in quantum information studies, just as its freezing cousin has already done [12].

3. Avoided crossings

If we add a variable bias to the symmetrical well, so that one side is deeper than the other, we can perform interesting numerical experiments in which the bias is slowly changed from one sign to the other. In the absence of the coupling to the thermal bath, a particle localized on one side can be permanently transported to the other side through an adiabatic reversal of sign of the bias. When moderate “side-blind” noise is added, we find that instead of the near 100% transportation of the uncoupled case we obtain a final distribution with approximately 50% of the probability on either side. However, in the presence of strong “side-blind” noise we find the efficiency of the transportation to be restored.

4. Quantum measurement

We discuss the connection between system-bath interactions and quantum measurement. We show that the system-apparatus-environment entanglement needed within the emerging paradigm for the description of quantum measurements can arise naturally in our context for the side-sensing case.

C. Structure of the paper

In section II we specify our system-bath Hamiltonian and the corresponding master equation for the system. We then discuss both the synchronized and frozen behavior and include an extension to the case of multi-particle systems with Fermi statistics. At the end

of this section we analyse the case of the double well with a time dependent bias, focussing on avoided level crossing transitions. In section III we determine the evolution of entangled well states under the influence of side-blind noise. We discuss the side-sensing and side-blind interactions from a measurement theoretic perspective in section IV and in section V we conclude.

II. DYNAMICS OF FREEZING VERSUS SYNCHRONIZATION

A. The master equation: single particle case

We focus on those situations where the effect of system-bath interactions on the dynamics of the system can be derived from a master equation for the reduced density matrix of the system.

The horizontal “spin” coordinate of the n -state system (where $n = 2$ for the double well) is indexed with Greek letters, while the vertical energy variables will be denoted E_i . The system basis states are denoted $|E_i, \alpha\rangle$. The dynamics of the system uncoupled to the bath is governed by the Hamiltonian,

$$H_0^{\text{sys}} = \sum_{i,\alpha,\beta} [E_i \delta_{\alpha\beta} + \lambda_{\alpha\beta}(E_i)] |E_i, \alpha\rangle \langle E_i, \beta|. \quad (1)$$

We will study the case $\lambda_{\alpha\beta}(E_i) \ll E_k$ for all values i, k . This means that the energy eigenstates fall into nearly degenerate pairs near each E_i , and the energy splittings within these pairs are always much smaller than the spacings ΔE between the pairs (single-well spacings).

Consider a reduced density matrix for the system $\rho^{\text{sys}}(t) = \text{Tr}_{\text{bath}}[\rho^{\text{s+b}}(t)]$, where $\rho^{\text{s+b}}(t)$ is the complete density matrix of the model. At an initial time $t = 0$ we choose a form diagonal in the vertical indices,

$$\rho^{\text{sys}}(t = 0) = \sum_{i,\alpha,\beta} \rho_{\alpha\beta}(E_i, t = 0) |E_i, \alpha\rangle \langle E_i, \beta|. \quad (2)$$

For these initial conditions, one of the results of a master equation derivation is that for times $t \gg (\Delta E)^{-1}$, the operator ρ^{sys} remains so nearly diagonal in the vertical (energy) indices that we can continue to describe the system by a vector in the energy space, $\rho(E_i, t)_{\alpha\beta}$, replacing $(t = 0)$ by (t) in Eq.(2). Henceforth we suppress the indices (α, β) in the horizontal space, in which $\rho(E_i, t)$ remains an operator.

We now have to supply a model for the system-bath interaction. A natural and simple case to consider is a factorised form,

$$H_{s-b} = \zeta V, \quad (3)$$

where ζ operates on the horizontal indices and V depends only on the vertical coordinates and the coordinates of the bath. This coupling is also taken to be weak, in a way that allows the problem to be solved, although it can at the same time be strong in another sense: we will eventually study the limiting case where the system-bath interaction rate is much larger than the free oscillation rates of the system.

In the Appendix, we show that for this form of coupling the master equations, generalized to include the vertical structure, are of the form,

$$\begin{aligned} \frac{\partial}{\partial t} \rho(E_i, t) = & -i[\lambda(E_i), \rho(E_i, t)] + \sum_j \zeta \rho(E_j, t) \zeta \Gamma(E_j, E_i) \\ & - \frac{1}{2} \left(\zeta^2 \rho(E_i, t) + \rho(E_i, t) \zeta^2 \right) \sum_j \Gamma(E_i, E_j). \end{aligned} \quad (4)$$

These equations are of Bloch form. All of the elements in Eq.(4) are matrices in the horizontal space except for the rate functions Γ . They obey the relation

$$\Gamma(E_j, E_i) = \exp[(E_j - E_i)/T] \Gamma(E_i, E_j) \quad (5)$$

due to the thermal equilibrium of the bath. For the neutrino application, and with the right identifications, Eq.(4) gives the ‘‘quantum kinetic equations’’ derived by McKellar and Thomson [13]. They can also be found in the NMR literature, for example in Ref. [11]. The derivation in the Appendix produces the equations in the context needed for our present results.

We now specialize to the symmetrical double well. The two-dimensional horizontal space consists of the left and right sides of the well, conveniently labelled by the eigenvalues of σ_3 , namely $+1$ (-1) for the particle to be on the left (right) side. The barrier height is chosen to be large compared to ΔE . The vertical states are the single well energy excitations. We take

$$\lambda_{\alpha\beta}(E_i) = [\sigma_1]_{\alpha\beta}g(E_i) \quad (6)$$

in order to model the free oscillations between left and right. The energy splittings $g(E_i)$, which are essentially tunneling rates, have strong E_i dependence. For the “spin” dependence of the coupling to the bath we take,

$$\zeta = 1 + b\sigma_3, \quad (7)$$

where the parameter b plays the important role of modelling the horizontal structure of the system-bath interaction. In the case $b = 0$, the transition matrix elements of the operator H_{s-b} for $E_i \rightarrow E_j$ in the left-hand well, considered by themselves, are the same as those for the right-hand well, as would be the case in the dipole approximation of the interaction with a radiation field. For the case $b = 1$ (-1), only the amplitude on the left-hand (right-hand) side of the well interacts with the bath. In other words, $b = 0$ (± 1) describes left-right symmetric (maximally asymmetric) system-bath couplings: side-blind (maximally side-sensing) in other words. As we review below, frozen behavior arises as a limiting case for $b \neq 0$ couplings, while synchronization or motional narrowing occurs as a limiting case when $b = 0$.

The function $\Gamma(E_i, E_j)$ is the (single well) rate for a state E_i to make a transition to state E_j . When $T \approx \Delta E$, the bath induced transitions among the vertical states are dynamically important. In this case our models differ substantively from models that do not have the vertical structure.

As an example we use a double square well with infinite barriers to the left and right of $x = \pm 8a$, and with a central barrier of width $2a$ and height U_0 . We choose U_0 and the

particle mass such that twenty states are bound with energies less than U_0 . The low-lying states are thus very nearly the symmetrical and anti-symmetrical combinations of separate states in an infinite well of width $7a$. The energy splittings, $g(E_i)$ are easy to calculate in the limit of small tunneling.

For the bath we take bosons with $\omega = vk$, equal energy spacing $2\pi v/L$ where $L \rightarrow \infty$, and with creation and annihilation operators, a_n^\dagger, a_n . We take

$$H_0 = \sum_n \omega_n a_n^\dagger a_n + H_0^{(\text{sys})}, \quad (8)$$

and in the system-bath interaction, $H_{s-b} = V\zeta$, we take the vertical operator V to have off-diagonal matrix elements given in dipole expansion as

$$V_{jk} = \frac{q}{L} \sum_n [(a_n^\dagger + a_n)\delta_{jk} + ik_n x_{jk}(a_n^\dagger - a_n)]. \quad (9)$$

where q is a coupling strength. We calculate the off-diagonal dipole matrix elements, x_{jk} , using the infinite well wave-functions and define $c_{jk} = qk_n x_{jk}$, where the later formalism will justify using (near) energy conservation to express k_n as $\pm(E_j - E_k)/v$. The transition rates in the bath interaction part of Eq.(4) are then,

$$\Gamma(E_k, E_j) = 2\pi c_{jk} c_{kj} \left[\frac{\theta(E_j - E_k)}{e^{(E_j - E_k)/T} - 1} + \frac{\theta(E_k - E_j)}{1 - e^{(E_j - E_k)/T}} \right]. \quad (10)$$

We will now display solutions to the master equations for the cases $b = 0$ and $b \neq 0$.

B. Results for $b = 0$: synchronization or motional narrowing

We first consider side-blind system-bath couplings, so that $b = 0$, and we solve Eq.(4) for several values of q^2 . The resulting curves are labeled with a ratio Q that is proportional to q^2 ,

$$Q \equiv \langle \Gamma \rangle / \langle g \rangle, \quad (11)$$

where $\langle g \rangle$ is the thermal average of the oscillation rates, $g(E)$, and $\langle \Gamma \rangle$ that of the bath induced transition rates, $\Gamma(E_j, E_k)$. Figure 1 shows the probability that a particle beginning

on the left side in a thermal distribution will be on the left side at time t . We choose temperature $T = 5$ in units of the single-well ground state energy.

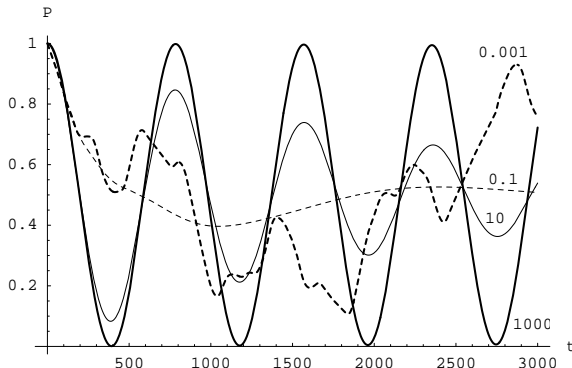


FIG. 1. The probability P for a particle to be found in the left hand well, for a bath temperature $T = 5$, in units of the ground state energy of the single infinite well. The initial condition is that the particle is on the left with a thermal distribution of energies. The curves are labelled by values of the rate-ratio parameter Q that range from 0.001 to 1000. The time is in an arbitrary unit, the scale of which is of the order of \hbar times the inverse of the single well energy spacings.

For the largest value of Q the probability shows undamped sinusoidal behavior in time. (This can be demonstrated in the $Q \rightarrow \infty$ limit analytically, with the result that the oscillation frequency is the thermal average of the oscillation frequencies for the separate modes [10]). For somewhat smaller values the probability settles rather quickly to 50%. For very small Q the probability shows the irregular behavior characteristic of the incommensurate frequencies $g(E_j)$. Note that arbitrarily large values of Q can be achieved for any value of system-bath coupling, q (whether the mechanism be photons, phonons or collisions with surrounding particles), by widening sufficiently the barrier between the wells.

In Fig. 2 we show the von Neumann entropy, as defined by

$$S = - \sum_j \text{Tr}\{\rho(E_j) \log[\rho(E_j)]\}, \quad (12)$$

where the trace is over the two-dimensional horizontal space. We note that as Q is increased from small to moderate values the rate of entropy increase rises, but that as Q becomes very large the rate of entropy increase goes to zero.

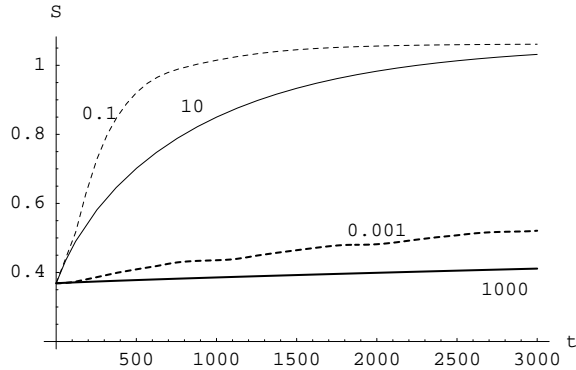


FIG. 2. The entropy S as a function of time for the same values of Q as used in fig.1. Time in arbitrary units.

Notice that the entropy begins at a nonzero value. This is simply due to our initial state being thermal with respect to the vertical variable. (If we had chosen a non-thermal state it would have been rapidly thermalized anyway in the large Q limit.) Any increase in S beyond this base level then reflects loss of order with respect to the horizontal variable, which is really what we are interested in.

C. Results for $b \neq 0$: freezing or quantum Zeno effect

We briefly summarize some examples. In the case plotted in Fig. 1, for the strongest coupling, we find little change for $b = 0.001$. But $b = 0.005$ starts to poison the oscillation, damping it by a factor of 20% in five periods. As we move to much larger b , the motion becomes more frozen, so that when, for example, $b = 0.5$, 98% of the probability has remained on the left hand side over a time span of five average periods of the $b = 0$ system. Thus side-sensing bath interactions are very efficient in freezing the time development.

The von Neumann entropy S shows qualitatively similar behavior to the $b = 0$ case. As we increase R , the entropy at first increases, but eventually it becomes frozen at its initial value when the QZE limit is reached. An important difference between the two cases is that entropy increase abates for $b = 0$ with the system evolving non-trivially with time, whereas

for $b \neq 0$ it freezes, simply because all evolution freezes.

D. Fermi statistics case

We presented the results for the previous sections in terms of the density matrix for a single particle in the well. If we choose to put several distinguishable particles in the same well and there are no interactions among these particles, then the results for each particle are the same as the previous results, and if we wished we could write a single equation for the density matrix for the assemblage, normalized to the number of particles. The same is true for the case of an assemblage of indistinguishable particles in the case that the temperature is high enough for Boltzmann statistics to obtain. For the N particle case with Fermi statistics, in the regime where the statistics matter, we have not succeeded in deriving an acceptable modification of Eq.(4). However, if we choose to use a formulation in which the diagonal matrix element of a density operator gives the probability that a state is occupied, and these occupancies are taken as independent ¹, there is a simple extension of Eq.(4) that describes the time evolution of the ensemble of fermions in the well. Following the argument of [14] we replace Eq.(4) by,

$$\begin{aligned} \frac{\partial}{\partial t} \rho(E_i, t) = & -i[\lambda(E_i), \rho(E_i, t)] + \\ & \frac{1}{2} \sum_j \left([1 - \rho(E_i, t)] \zeta \rho(E_j, t) \zeta + \zeta \rho(E_j, t) \zeta [1 - \rho(E_i, t)] \right) \Gamma(E_j, E_i) \\ & - \frac{1}{2} \sum_j \left(\zeta [1 - \rho(E_j, t)] \zeta \rho(E_i, t) + \rho(E_i, t) \zeta [1 - \rho(E_j, t)] \zeta \right) \Gamma(E_i, E_j). \end{aligned} \quad (13)$$

The density matrix is now to be normalized to the average number of particles, $\sum_j \text{Tr}[\rho(E_j, t)] = \langle N \rangle$, which is time independent. As an example we take a system which begins at $t = 0$ with no particles on the RHS, and an average number of particles $\langle N \rangle = 8$ on the LHS, for a well system with the same parameters used to generate data for the single

¹When the occupancies are taken as independent, the particle number is necessarily indeterminate.

particle calculation. For the initial energy distribution we take 50% occupancy for each of the lowest sixteen states.

In the case of zero coupling to the thermal bath, the various particles rattle back and forth independently with their incommensurate frequencies. Our terminology has been changed here, since previously we pictured the density matrix for a single particle performing exactly the same gyrations. We note that in the case without vertical transitions the Fermi statistics enter only in the restrictions put on the initial state.

In the presence of a moderate coupling to the bath, the system tends rather quickly to an equilibrium state with 50%-50% L-R occupancy, as shown in the heavy dashed curve in Fig. 3. In this state the final energy distribution is a Fermi function,

$$\rho(E_j, t) = [1 + e^{(E_j - \mu)/T}]^{-1} \quad (14)$$

where the parameter μ is set by

$$2 \sum_j [1 + e^{(E_j - \mu)/T}]^{-1} = \langle N \rangle \quad (15)$$

But, as before, if we increase the bath coupling sufficiently, the particle density oscillates back and forth sinusoidally as shown in the heavy solid curve of Fig. 3. The average frequency is now given by the average of the individual-state rates with respect to the Fermi distribution function. We have not found in the literature an analogue of this behavior, in which a group of fermions undergoes collective synchronized oscillations, as though they were all in the same state.

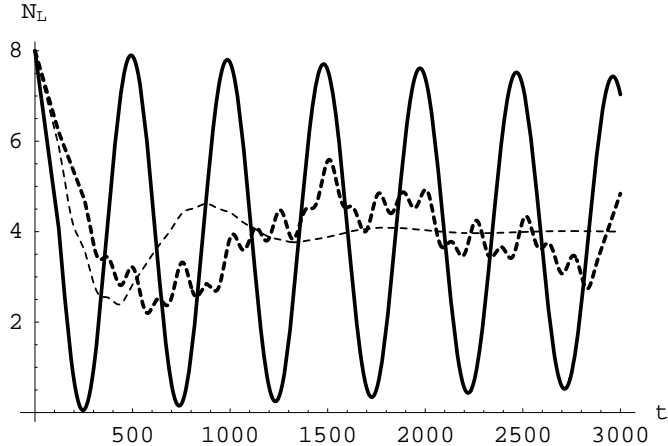


FIG. 3. The time development of the average number of particles in the left hand well. The initial conditions are: the first sixteen levels of the left well each occupied with 50% probability. The heavy dashed curve gives the behavior with extremely small coupling to the bath, the lighter dashed curve the behavior with an intermediate value of the coupling, and the heavy solid curve the behavior with the largest coupling. The respective couplings are in the ratios of 10^{-3} , 1, and 10^3 . The time is in arbitrary units.

E. Adiabatic inversion

A generalization of the above considerations is the extension to a double well with a time dependent bias,

$$\delta H_0^{\text{sys}} = \epsilon(t)\sigma_3. \quad (16)$$

Consider a case in which we begin with $\epsilon > 0$ and $\epsilon \gg |g(E_i)|$ for some set of low-lying states (but $\epsilon \ll \Delta E$). A particle not interacting with the medium, initially localized on the left, with its density matrix distributed among the low-lying states, will stay largely on the left as long as the bias is maintained at the initial value. If the bias is slowly lowered, going through zero and ending at the negative of the original value, then the particle will efficiently be carried to the right hand well. The mechanism can be described as “avoided

crossing".² Now we consider the same process in the presence of a side-blind thermal bath. With a moderate coupling to the bath, the system will still remain localized on the left if we keep the bias constant at its initial large value. But if we proceed as before through an adiabatic reversal of the bias, then the jostling caused by the vertical transitions will reduce the efficiency of the left to right transportation, and will tend to leave one-half of the probability behind in the left hand well.

However, if we increase the strength of the bath coupling sufficiently, then we regain the efficient shift from left to right.³ Figure 4 shows the results of the calculation, for the cases of no bath coupling, moderate bath coupling and strong bath coupling. Note that in this example the transport of the particle from the left to right is even more efficient in the case of large bath coupling than it was in the case of no bath coupling, the small inefficiency caused by some non-adiabaticity in the bias-changing process being reduced in the presence of the bath coupling.

This rather surprising behavior can perhaps be understood qualitatively in the following way: First consider the previously discussed synchronized oscillation limit for the symmetrical well. There the synchronized frequency is somewhat higher than we would have guessed from the oscillation frequency for a typical particle (with $E \approx T$) in the absence of the bath, because in our model the tunnelling rates increase rapidly as we move up in energy. It is also true that the non-adiabaticity, as defined by the fraction of particles ending up on the left at the end of our bias-reversal, declines rapidly with increasing energy, again in the absence of bath interactions. Thus the bath's effects, still a bit mysterious, are to use the synchronized frequency for the purpose of the estimation of adiabaticity. We emphasize that

²This is the analogue of the Mikheyev-Smirnov-Wolfenstein (MSW) [15] transition in neutrino physics. This behavior is addressed in [8] for the case of a thermal bath that does distinguish the right and left sides of the well. As expected, their results are quite different for the case of large Q .

³Detailed analysis of similar behavior for a neutrino application is given in [10].

the real energy distribution of the particles remains very nearly thermal; but synchronization lets us do the tunnelling, in effect, at a higher energy, with consequent smaller inefficiency.

This phenomenon offers some promise for obtaining greater L-R transition efficiency in an application. Another example of parameters, beyond the ones presented in Fig. 4 is the following: take the temperature so low that the occupancy of the ground state is 97%, the first excited state, 3% and the higher states negligible. Then we find, for a particular rate of bias inversion and a particular level of coupling to the bath, that there is 6% probability to end in the left hand well. This is to be compared to 16% in the absence of the bath coupling.

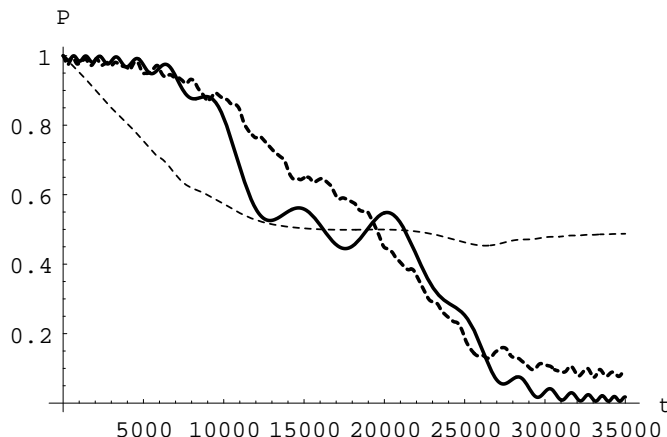


FIG. 4. The probability that the particle is on the left, where the well bias is reversed. The heavy dashed curve is for zero system-bath coupling, the light dashed curve for moderate coupling and the solid curve for large coupling. The time is in arbitrary units. (The dependence of ϵ on t has been taken to be proportional to $(t - t_0)^3$, where t_0 is the zero-bias time.)

III. EVOLUTION OF ENTANGLEMENT

Irrespective of the value of b , we have concluded that the quantum coherence of a state that is initially a left or right eigenstate (with a thermal distribution of energies) is preserved under time evolution in the $Q \rightarrow \infty$ limit. For $b \neq 0$, this is because of freezing, while for $b = 0$ coherence manifests as motional narrowing or synchronization.

It is natural to then ask whether entanglement is preserved in the same limit. For the QZE case, the answer is no, simply because any L-R entangled state has off-diagonal entries that are rapidly damped when $b \neq 0$. In other words, entanglement will be destroyed, not frozen, in the QZE limit. We now want to see what happens in the synchronization case. Intuitively, one expects preservation to be maintained because all components of the entangled multi-particle system will oscillate between the wells at the same rate.⁴ This intuition is borne out by direct computation.

We will focus on bipartite or two-particle states for simplicity. The maximally entangled or Bell states are

$$\begin{aligned} |\Psi^\pm, E_i, E_j\rangle &\equiv \frac{|E_i, L\rangle \otimes |E_j, R\rangle \pm |E_i, R\rangle \otimes |E_j, L\rangle}{\sqrt{2}}, \\ |\Phi^\pm, E_i, E_j\rangle &\equiv \frac{|E_i, L\rangle \otimes |E_j, L\rangle \pm |E_i, R\rangle \otimes |E_j, R\rangle}{\sqrt{2}}, \end{aligned} \quad (17)$$

where one well particle has energy E_i and the other energy E_j .

A straightforward generalisation of the derivation sketched in the Appendix yields the master equation for a general two-particle system. We denote the basis states of the system as $|E_i, E'_j, \alpha, \beta\rangle$ and consider a density matrix (diagonal in the two energy spaces) $\rho(E_i, E'_j)_{\alpha, \alpha', \beta, \beta'}$.

Suppressing the flavor (R-L) matrix indices, the Bloch equations, generalized to include the vertical structure, are of the form,

$$\begin{aligned} \frac{d}{dt}\rho(E_i, E_j, t) &= -i[\lambda(E_i), \rho(E_i, E_j, t)] - i[\lambda'(E_j), \rho(E_i, E_j, t)] \\ &+ \sum_{E_k} \zeta \rho(E_k, E_j, t) \zeta \Gamma(E_k, E_i) + \sum_{E_m} \zeta' \rho(E_i, E_m, t) \zeta' \Gamma(E_m, E_j) \\ &- \frac{1}{2} \left(\zeta^2 \rho(E_i, E_j, t) + \rho(E_i, E_j, t) \zeta^2 \right) \sum_{E_j} \Gamma(E_i, E_k) \\ &- \frac{1}{2} \left((\zeta')^2 \rho(E_i, E_j, t) + \rho(E_i, E_j, t) (\zeta')^2 \right) \sum_{E_m} \Gamma(E_j, E_m). \end{aligned} \quad (18)$$

⁴Note that synchronization preserves coherence given any initial state, as opposed to the QZE which preserves coherence only if the initial state is an eigenstate of σ_3 .

Here $\lambda(E)$, $\lambda'(E)$, ζ , and ζ' are matrices in the (R-L, R-L) space. For the case of symmetric double wells, the only horizontal matrices in the free oscillation part of the Hamiltonian are constructed from the σ_1 matrices of the two particles and we have

$$\begin{aligned}\lambda_{\alpha\alpha'\beta\beta'}(E) &= g(E)[\sigma_1]_{\alpha\alpha'}\delta_{\beta\beta'}, \\ \lambda'_{\alpha\alpha'\beta\beta'}(E') &= g(E')\delta_{\alpha\alpha'}[\sigma_1]_{\beta\beta'}.\end{aligned}\tag{19}$$

It is useful to parametrise the the density matrix in terms of the coefficients x_{ij} in an expansion in terms of sigma matrices

$$\rho = x_{ij}(E, E')\sigma_i \otimes \sigma_j.\tag{20}$$

If we choose as our initial condition one of the four Bell states in eq.(17), we need consider only the six components $x_{00}, x_{11}, x_{22}, x_{23}, x_{32}$ and x_{33} . If, additionally, the initial state is one of thermal equilibrium with respect to the vertical variables then $x_{00}(E, E')$ and $x_{11}(E, E')$ remain constant and we are left with the four equations

$$\begin{aligned}\frac{d}{dt}x_{ij}(E, E') &= g(E)\sum_k \xi_{ik}x_{kj}(E, E') + g(E')\sum_k \xi_{jk}x_{ik}(E, E') \\ &+ \sum_{E_k} \left[x_{i,j}(E_k, E'_j, t)\Gamma(E_k, E_i) - x_{ij}(E_i, E'_j, t)\Gamma(E_i, E_k) \right] \\ &+ \sum_{E'_m} \left[x_{ij}(E_i, E'_m, t)\Gamma(E'_m, E'_j) - x_{ij}(E_i, E'_j, t)\Gamma(E'_j, E'_m) \right],\end{aligned}\tag{21}$$

where the nonvanishing elements of the matrices ξ are $\xi_{32} = -\xi_{23} = 2$. In eq.(21) we have specialised the collision terms to the case $\zeta = \zeta' = 1$, in which the system-bath couplings do not distinguish the value of the (L,R) index.

We quantify the degree of entanglement using the *entanglement of formation* [16]. For a bipartite system, the entanglement of formation is given by

$$E_f(C) = h\left(\frac{1}{2} + \frac{1}{2}\sqrt{1 - C^2}\right),\tag{22}$$

where

$$h(x) = -x \log_2 x - (1 - x) \log_2(1 - x).\tag{23}$$

The ‘‘concurrence’’ C is

$$C = \max\{0, \lambda_1 - \lambda_2 - \lambda_3 - \lambda_4\}, \quad (24)$$

where the λ_i are the square roots of the eigenvalues of the matrix $\rho\tilde{\rho}$, and the spin-flipped state $\tilde{\rho}$ is defined as

$$\tilde{\rho} = (\sigma_y \otimes \sigma_y)\rho^*(\sigma_y \otimes \sigma_y). \quad (25)$$

We illustrate the evolution of the entanglement in the figures below, for the side-blind case with the initial conditions $|\Phi^\pm(E_1, E_1)\rangle$. In the absence of the heat bath, a system initially in the state $|\Phi^-(E_1, E_1)\rangle$ will remain in that state. An initial state of $|\Phi^+(E_1, E_1)\rangle$, however, evolves as $|\psi(t)\rangle = \cos[2g(E_1)t]|\Phi^+(E_1, E_1)\rangle - i\sin[2g(E_1)t]|\Psi^+(E_1, E_1)\rangle$ in the absence of a heat bath, while, of course, maintaining maximal entanglement.

In Figs. 5 and 7 we plot the evolution of X_{33} ,

$$X_{33} = 2 \left(0.25 + \sum_{i,j} x_{33}(E_i, E_j) \right), \quad (26)$$

which measures the probability that if one of the particles is on the left (right), the other particle will also be found on the left (right). In Figs. 6 and 8 we plot the entanglement of formation, calculated after first summing over the vertical states

$$\rho = \sum_{i,j} \rho(E_i, E_j). \quad (27)$$

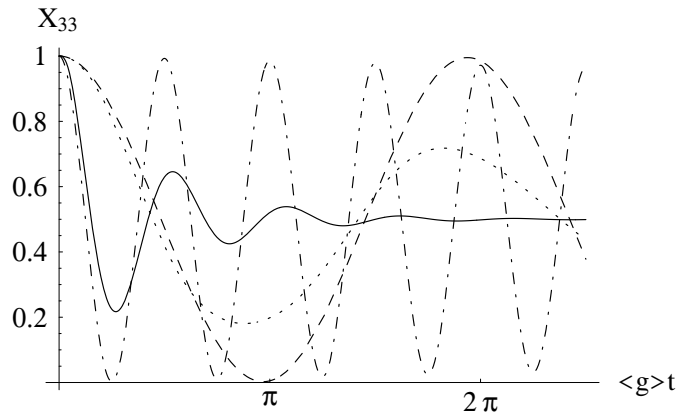


FIG. 5. The evolution of X_{33} as a function of time, for the initial state $|\Phi^+(E_1, E_1)\rangle$. The dashed, dotted, solid and dot-dashed curves are for $Q = 0.0005, 0.05, 5$ and 500 respectively.

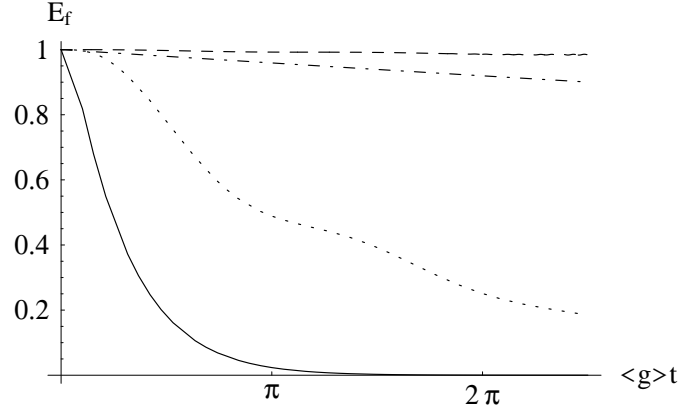


FIG. 6. The entanglement of formation, E_f , for the same parameters as Fig.5.

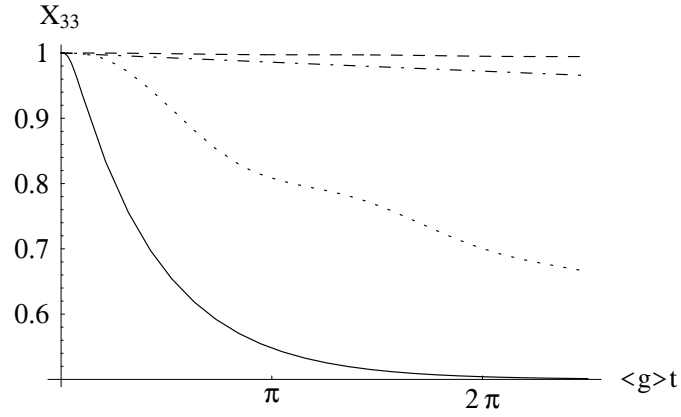


FIG. 7. The evolution of X_{33} as a function of time, for the initial state $|\Phi^-(E_1, E_1)\rangle$. The values of the parameter Q are as in Fig.5.

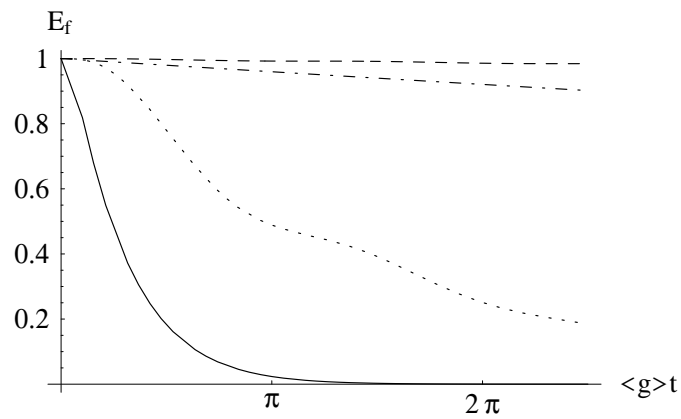


FIG. 8. The entanglement of formation, E_f , for the same parameters as in Fig.7.

For small to moderate Q values, we observe the gradual relaxation and decay of entanglement arising from the population of energy levels with different frequencies. For large values of Q , we obtain synchronised behaviour, where the evolution of the system resembles that of two isolated qubits, with $\lambda(E_1)$ replaced by an averaged frequency $\bar{\lambda}$. That is, despite the strong coupling to the bath, the system behaves, effectively, as though it were isolated. In the limit $Q \rightarrow \infty$, we see the persistence of maximal entanglement.

Finally, note that entanglement may be created or destroyed if the Hamiltonian were to have a term describing an interaction between the two qubits. In the large Q limit this process will also proceed as if the system were isolated, with the Hamiltonian parameters replaced by their averaged values.

IV. DISCUSSION

The freezing phenomenon or QZE is well known. It should be noted, though, that much of the recent non-neutrino literature does not study systems with a vertical structure. Indeed, when the vertical structure is removed Eq.(4) reduces to the familiar form,

$$\frac{\partial \rho}{\partial t} = -i[\lambda, \rho] - \frac{\Gamma}{2}[\zeta, [\zeta, \rho]]. \quad (28)$$

The decoherence term is then simply

$$\frac{\Gamma}{2}[\zeta, [\zeta, \rho]] = -2b^2\Gamma \begin{pmatrix} 0 & \rho_{12} \\ \rho_{12}^* & 0 \end{pmatrix}, \quad (29)$$

from which freezing can be deduced in the large Q limit, provided that $b \neq 0$. The presence of vertical states evidently does not alter these qualitative conclusions: freezing occurs at large Q for $b \neq 0$ whether vertical structure exists or not.

The above derivation also shows that $b = 0$ system-bath interactions have no affect on the system in the absence of vertical structure. But, when it is not absent, we have seen that

there is an interesting conceptual cousin to the $b \neq 0$ quantum Zeno effect: synchronization (or motional narrowing) when $b = 0$.⁵ Both occur in the $Q \rightarrow \infty$ limit, when the dynamics of the system is dominated by its interactions with the bath. While synchronization from motional narrowing is a known phenomenon, we have not found a clear and comprehensive discussion in the literature about its relationship with the QZE, quantal coherence and measurement, so we now provide one.

The strong connection between freezing/synchronization and coherence is revealed by the evolution of entropy. Pure states always have vanishing entropy. Decoherence in the system induced by system-bath interactions can cause initially pure states to evolve into mixed states. In this case the entropy increases towards a maximum which is attained when all states in the statistical mixture are equally populated, with complete decoherence.

We have to be careful to distinguish between what one may call vertical and horizontal contributions to entropy. As explained when we discussed Fig. 2, the entropy of our system starts out being nonzero because of the thermalization in the vertical variable. We are really interested in whether or not S increases from this initial offset, because that change would be caused by growing horizontal disorder. But we have seen that a system initially in a horizontal eigenstate experiences no entropy increase for any value of b in the large Q limit. This means that the system evolves in a pure-state manner (subtracting off the initial vertically induced offset), despite having its dynamics dominated by interactions with the bath: environmental decoherence hits a maximum at an intermediate value of Q , not in the limit $Q \rightarrow \infty$. For $b \neq 0$, this is in a sense Pyrrhic victory over decoherence since it comes at the cost of freezing. For $b = 0$ on the other hand, the ensemble described by the reduced density matrix evolves nontrivially as if it were a single isolated particle undergoing unitary evolution at an averaged frequency.

⁵Of course this manifests itself only when the vertical coordinate exists because one cannot talk about synchronization for a one-oscillator system!

Whether freezing or synchronization results in the large Q limit depends on how the bath couples to the system. If the bath is side-sensing, ($b \neq 0$) then freezing happens; if it is side-blind ($b = 0$), then synchronization occurs. It has often been remarked that the QZE case is connected with the measurement process. Since the environment has a $b \neq 0$ coupling, it can “tell the difference” between left and right sides of the well, and thus “measure” this observable (the Hermitian operator σ_3). When $Q \rightarrow \infty$, the system-bath “measurement” interactions happen repeatedly and quickly (constant monitoring), forcing the system to remain in the same σ_3 eigenstate (or more generally to remain in the same statistical mixture of eigenstates). On the other hand, if the coupling is of $b = 0$ form, then there is no sense in which the environment probes whether the system is in the left or right state, and therefore it cannot “measure” and thus freeze σ_3 . The oscillations between left and right are undamped, but the system states transform between vertical E_i levels so rapidly that they effectively all oscillate at the same averaged frequency.

These are heuristic observations, as indicated by the scare quotes around key phrases and words. It would be useful to make the connection between b and measurement more rigorous. This should be possible in light of the recent clarification of how exactly measurement can be modeled in quantum theory.

The emerging paradigm connects the measurement process to entanglement between system, apparatus and environment states [4]. We will see that microscopic collisions between a system particle and a spin-0 boson from the bath can be interpreted as inducing this sort of entanglement in the $b \neq 0$ case.⁶ So, the microscopic perspective will provide us with a simple explanation for why the $b \neq 0$ and $b = 0$ cases are different, and indeed why the former is connected with measurement. These considerations will not capture the full complexity of the phenomena generated by the master equations (synchronization in particular),

⁶System-environment entanglement should not be confused with the intra-system entanglement studied in Sec.III.

but they will furnish some physical insight.

We first briefly summarize the emerging paradigm. The world is divided into three parts: system, apparatus and environment. Suppose that the system is initially in state $|\mathcal{S}\rangle = \sum_n c_n(0)|n\rangle$, where $|n\rangle$ is an eigenstate of O , the system observable that the apparatus can measure. Initially, we take the apparatus and environment to be in states $|\mathcal{A}\rangle$ and $|\mathcal{E}\rangle$, respectively. We also suppose that initially there are no correlations between the three subsystems, so the state of the world begins as simply $|\mathcal{S}\rangle \otimes |\mathcal{A}\rangle \otimes |\mathcal{E}\rangle$. By time t_1 , the system and apparatus have unitarily evolved into the entangled state $\sum_n c_n(t_1)|n\rangle \otimes |a_n\rangle$, so that a correlation now exists between eigenstates of the system $|n\rangle$ and some basis states $|a_n\rangle$ for the apparatus. In the typical picture, the environment at this “pre-measurement” stage remains uncorrelated with the system-plus-apparatus hybrid. The measurement is not complete at this stage because quantal correlations exist between the “outcomes”. By time t_2 , however, we suppose that unitary evolution has also entangled the environment with the apparatus, in a way such that each apparatus state $|n\rangle$ is linked to a distinct environmental state, $|e_n\rangle$. Now the world is in the fully correlated state

$$\sum_n c_n(t_2)|n\rangle \otimes |a_n\rangle \otimes |e_n\rangle. \quad (30)$$

The final step is to argue that the environment states $|e_n\rangle$ are by definition inaccessible or uninteresting, so one should trace over them to obtain the reduced density matrix for system-plus-apparatus. Doing this we obtain

$$\rho_{\text{s+a}}(t_2) = \sum_n |c_n(t_2)|^2 |n; a_n\rangle \langle n; a_n|, \quad (31)$$

where we have taken the environment states to be orthonormal, and we have defined $|n; a_n\rangle \equiv |n\rangle \otimes |a_n\rangle$. This reduced density matrix describes a mixture of states which have *classically* correlated system-apparatus variables. The measurement is complete, with all *quantal* correlations between system and apparatus having diffused into the environment, thus effectively becoming lost.

We will now connect this schematic to our case by examining a microscopic energy-changing collision between a system particle and a spin-0 bath boson ϕ . We previously called

the Hilbert space spanned by the horizontal *and* vertical states as the “system”. It is now useful to change perspective. Let us redefine “system” to mean the Hilbert space spanned by just the horizontal eigenstates (left or right), with the “apparatus” being spanned by the vertical states (single well energy eigenstates labeled by E). The environment is spanned by the energy states $|e\rangle$ of ϕ .

The initial state is

$$[c_1(0)|L, E\rangle + c_2(0)|R, E\rangle] \otimes |e\rangle, \quad (32)$$

the left and right eigenstates being

$$\begin{aligned} |L, E\rangle &= \frac{|E + \omega\rangle + |E - \omega\rangle}{\sqrt{2}}, \\ |R, E\rangle &= \frac{|E + \omega\rangle - |E - \omega\rangle}{\sqrt{2}}, \end{aligned} \quad (33)$$

respectively, where $E \pm \omega$ label the nearly degenerate double-well states collectively indexed by the vertical designation E . Free unitary evolution takes the initial state in Eq.(32) to

$$e^{-i(E+e)t} [c_1(t)|L, E\rangle + c_2(t)|R, E\rangle] \otimes |e\rangle \quad (34)$$

at time t , where $c_{1,2}(t) = c_{1,2}(0) \cos \omega t - i c_{2,1}(0) \sin \omega t$. We will ignore the unimportant overall phase factor in the following. Suppose a collision with a bath boson occurs at the time t (we are assuming that the interaction time is very short compared to the mean free path). For simplicity, consider the extreme case $b = 1$ so that only L states interact with ϕ , and work in one spatial dimension. The latter idealisation, which is inessential, leads to the final energies being completely determined by kinetic energy and momentum conservation from the initial energies E and e . Immediately after the collision, the state of the system is

$$c_1(t)|L, E'\rangle \otimes |e'\rangle + c_2(t)|R, E\rangle \otimes |e\rangle, \quad (35)$$

where $E' \neq E$ and $e' \neq e$.⁷ This is already in the fully entangled form of Eq.(30); there

⁷In addition, the oscillation frequency has changed from ω to ω' for the left eigenstate.

is no distinct pre-measurement step. We now trace over the ϕ energy states to obtain the reduced density matrix

$$|c_1(t)|^2|L, E'\rangle\langle L, E'| + |c_2(t)|^2|R, E\rangle\langle R, E|. \quad (36)$$

In the sense made precise by the comparison of the above simple argument with the general schema, the measurement of the horizontal variable is complete.

On the other hand, if $b = 0$, then Eq.(35) is replaced by

$$[c_1(t)|L, E'\rangle + c_2(t)|R, E'\rangle] \otimes |e'\rangle, \quad (37)$$

whose reduced density matrix is that for the pure state $c_1(t)|L, E'\rangle + c_2(t)|R, E'\rangle$. There is no entanglement with the environment. The horizontal quantity remains unmeasured, even though there has been an energy changing collision with a bath boson.

It is interesting that it makes sense to consider the vertical states as spanning an apparatus which measures the horizontal states. We began by considering a three-part division of the world (horizontal, vertical, bath) for other reasons, but apparently this same partition provides a framework for interpreting aspects of the $b \neq 0$ dynamics as a canonical measurement process. Indeed, our master equation incorporating both horizontal and vertical states then precisely specifies the dynamics of what can be interpreted as a system-plus-apparatus hybrid.

We can sharpen this point. Suppose we put some particles into one of the energy eigenstate of an isolated well. They oscillate between the left and right states at a given frequency. At time t_{bath} (bath time) suddenly immerse it in a $b = 1, Q \rightarrow \infty$ bath. If the particles' phases happen to place them entirely in the left state at this time, then the system quickly becomes thermalised in energy and frozen in the left eigenstate. Now remove the system from the bath. If a thermalised distribution of oscillating particles is seen, then we know that the horizontal state was measured to be "left". On the other hand, if the phases at t_{bath} happen to place all of the particles in the right eigenstate, then the system will remain unchanged in energy but frozen in the right eigenstate. Upon removal from the bath, we see a non-thermalised distribution and hence we know the measurement yielded "right".

V. CONCLUSION

We have analysed behaviors that can be exhibited by a quantum system that is coupled to a thermal bath. The system states were taken to have both a horizontal and a vertical structure. The horizontal states are discrete and the system is generally in a superposition of them. Familiar examples are the left and right sides of a symmetrical double well, the case we focussed on, and neutrino flavor. The vertical states are labeled by the energy eigenvalues. A “dynamical superselection rule” induced by decohering interactions with the bath quickly eliminates superpositions in the vertical direction. However, the same system-bath coupling induces system transitions between the vertical states. The limit where the system-bath interaction rates were much larger than the free oscillation rates of the system was our particular concern.

Two qualitatively different, but complementary, limiting cases were analysed. The frozen or quantum Zeno case arises when the system-bath interactions distinguish between the horizontal states (side-sensing). The synchronized or motionally narrowed case arises, by contrast, when the system-bath interactions are blind to the horizontal structure (side-blind). The latter can only be observed when the vertical structure is present, whereas the former obtains even when the system is vertically trivial. Two extensions were made: to a double-well containing fermions, where the effect of Fermi statistics was fully incorporated into the master equation; and to potentials with a time-dependent bias. In the synchronization limit, the multi-fermion system presents a behavior which gives the illusion that all of the fermions are in the same state, evolving coherently. When there is a time-dependent bias, the synchronization limit can lead to an increase in the efficiency of transformation from one horizontal state into the other.

We then examined the time evolution of bipartite entanglement-of-formation in the face of side-blind system-bath interactions. Entanglement was observed to at first decrease with increasing system-bath coupling strength. However, when the synchronization limit was reached, entanglement was found to be preserved.

The connection between freezing/QZE on the one hand, and synchronization/motional-narrowing on the other, and measurement was clarified. By adopting the emerging “system + apparatus + environment” paradigm for quantal measurement, we were able to show that microscopic energy-changing interactions between a system particle and a bath boson can be naturally interpreted as measurement events in the horizontal observable. The tripartite subdivision “horizontal + vertical + bath” was mapped on to “system + apparatus + environment” in the process.

In closing, we would like to note that the synchronization or motional narrowing limit should be useful in applications such as quantum computation which exploit quantal coherence and entanglement. The experimental or engineering challenge would be to construct devices whose active or horizontal system elements are deliberately placed in a noisy environment, but one that couples to all horizontal states equally strongly.

ACKNOWLEDGMENTS

The work of R.F.S. was supported, in part, by NSF grant PHY-9900544, N.F.B. by the Commonwealth of Australia and the Australian Research Council, and R.R.V. by the Australian Research Council. We thank Y. Y. Y. Wong for helpful discussions.

-
- [1] A. J. Leggett, S. Chakravarty, A.T. Dorsey, M.P.A. Fisher, A. Garg, and W. Zwerger, *Rev. Mod. Phys.* **59**, 1 (1987) and references therein.
 - [2] For an overview see M. A. Nielsen and I. L. Chuang, *Quantum computation and quantum information*, Cambridge University Press (2000).
 - [3] For recent reviews see M. Prakash, J. M. Lattimer, R. F. Sawyer and R. R. Volkas, *Ann. Rev. Nucl. Part. Sci.* (in press, 2001), astro-ph/0103095; P. Di Bari, R. Foot, R. R. Volkas and Y. Y. Y. Wong, *Astropart. Phys.* **15**, 391 (2001).

- [4] See, for example, W. H. Zurek, *Physics Today* **44** (October) 36 , (1991); quant-ph/0105127; J. P. Paz and W. H. Zurek, Proceeding of the 72nd Les Houches Summer School on “Coherent Matter Waves”, July-August 1999, quant-ph/0010011; Roland Omnès, *Understanding quantum mechanics*, Princeton University Press (1999); D. Giulini et al., *Decoherence and the appearance of a classical world in quantum theory*, Springer (1996).
- [5] B. Misra and E. C. G. Sudarshan, *J. Math. Phys.* **18**, 756 (1977).
- [6] R. A. Harris and L. Stodolsky, *Phys. Lett.* **116B**, 464 (1982);
- [7] R. A. Harris and R. Silbey, *J. Chem. Phys.* **78**, 7330 (1993)
- [8] P. Silvestrini and L. Stodolsky, *Phys. Lett.* **A280**, 17 (2001); P. Silvestrini and L. Stodolsky, cond-mat/0010129.
- [9] L. Stodolsky, *Phys. Rev.* **D36**, 2273 (1987). See also A. Dolgov, *Sov. J. Nucl. Phys.* **33**, 700 (1981); K. Enqvist, K. Kainulainen and J. Maalampi, *Nucl. Phys.* **B 349**, 754 (1991).
- [10] N. F. Bell, R. F. Sawyer and R. R. Volkas, *Phys. Lett.* **B500**, 16 (2001).
- [11] A. Abragam, *The principles of nuclear magnetism*, Oxford (1961), ch. 10. See also Eberly et al., *Phys. Rev.* **A30**, 2381 (1984) for a “motion narrowing” effect in optics.
- [12] W. H. Zurek, *Phys. Rev. Lett.* **53**, 391 (1984); W. Y. Hwang et al., *Phys. Rev.* **A 62**, 062305 (2000), and references therein.
- [13] B. H. J. McKellar and M. J. Thomson, *Phys. Rev.* **D49**, 2710 (1994).
- [14] G. Raffelt, G. Sigl, and L. Stodolsky, *Phys. Rev. Lett.* **70**, 2363 (1993). See also G. Raffelt and G. Sigl, *Astropart. Phys.* **1**, 165 (1993).
- [15] L. Wolfenstein, *Phys. Rev.* **D17**, 2369 (1978); *ibid.* **D20**, 2634 (1979); S. P. Mikheyev and A. Yu. Smirnov, *Nuovo Cimento* **C9**, 17 (1986). For a review see e.g. T. K. Kuo and J. Pantaleone, *Rev. Mod. Phys.* **61**, 937 (1989).

- [16] S. Hill and W. K. Wootters, Phys. Rev. Lett. **78**, 5022 (1997); W. K. Wootters, Phys. Rev. Lett. **80**, 2245 (1998).
- [17] N. G. van Kampen *Stochastic Processes in Physics and Chemistry* North Holland (Amsterdam, 1992) (revised and enlarged edition), ch. XVII; D. F. Walls and G. C. Milburn, *Quantum Optics*, Springer (Berlin, 1994), ch. 6.

APPENDIX A: DERIVATION OF THE MASTER EQUATIONS

We provide a derivation of the master equations appropriate for the context of this paper. We focus on the aspects that give rise to the placing of the horizontal matrices in Eq.(4) and the detailed form of the right hand side of Eq.(10). The methods are closely related to those given in [17] but we employ no Markov approximation. We introduce an interaction picture based on the above division of the Hamiltonian. The system-bath coupling in this picture is denoted by $H_I(t)$, with vertical matrix elements,

$$[H_I(t)]_{j,k} = e^{i\lambda(E_j)t} \zeta e^{-i\lambda(E_k)t} V_{j,k}^I e^{i(E_j-E_k)t}. \quad (\text{A1})$$

The leading terms in the system+bath density matrix, ρ_I^{s+b} , in this interaction picture are generated by the integral equation,

$$\begin{aligned} \rho_I^{s+b}(t) &= \rho^{s+b}(t=0) \\ &\quad - \int_0^t dt_1 \int_0^{t_1} dt_2 [\rho_I^{s+b}(t_2), H_I(t_2)], H_I(t_1)]. \end{aligned} \quad (\text{A2})$$

In the perturbation expansion of Eq.(A2) we find a piece with an additional power of the quantities $c_{j,k}^2[Et, E\lambda^{-1}]$ in each higher order. This provides our definition of leading terms and the explanation for how a tiny $c_{j,k}^2$ can lead to appreciable effects over long periods of time. These terms are generated by the terms in which each successive new pair of H_I 's in the iteration solution puts the state back to the same vertical (and bath) state. These observations provide the basis for having omitted, in writing Eq.(A2), all odd terms in H_I , and they also dictate the form of the density matrix to be used in solving the equation,

$$\rho_I^{\text{s+b}} = \rho^{\text{bath}} \sum_j \rho_I(E_j, t) |j\rangle \langle j|. \quad (\text{A3})$$

where,

$$\rho^{\text{bath}} = \left[\prod_i (1 - e^{-\omega_i/T}) \right] \exp \left[- \left(\sum_n a_n^\dagger a_n \omega_n \right) / T \right], \quad (\text{A4})$$

and where,

$$\rho_I(E_j, t) = e^{i\lambda(E_j)t} \rho(E_j, t) e^{-i\lambda(E_j)t}. \quad (\text{A5})$$

We substitute Eq.(A3) into Eq.(A2), take the bath trace, and use leading order expressions for each term in the double commutator, obtaining, for example,

$$\begin{aligned} & \text{Tr}_{\text{bath}} \left[\langle j | H_I(t_1) \rho_I^{\text{s+b}}(t_2) H_I(t_2) | j \rangle \right] = \delta(t_1 - t_2) \\ & \times \sum_k \Gamma(E_k, E_j) e^{i\lambda(E_j)t_1} \zeta e^{-i\lambda(E_k)t_1} \\ & \times \rho_I(E_k, t_1) e^{i\lambda(E_k)t_1} \zeta e^{-i\lambda(E_j)t_1}. \end{aligned} \quad (\text{A6})$$

Similarly, we have

$$\begin{aligned} & \text{Tr}_{\text{bath}} \left[\langle j | H_I(t_1) H_I(t_2) \rho_I^{\text{s+b}}(t_2) | j \rangle \right] = \delta(t_1 - t_2) \\ & \times e^{i\lambda(E_j)t_1} \zeta^2 e^{-i\lambda(E_j)t_1} \sum_k \Gamma(E_j, E_k) \rho_I(E_j, t_1). \end{aligned} \quad (\text{A7})$$

The key to separation of the leading terms in the above is performing the sum over the modes of the scalar field first. After making the transition to the continuum, we make replacements of the form,

$$\begin{aligned} & \int_{\omega_{\text{min}}}^{\infty} d\omega f(\omega) e^{i(\pm E_j \mp E_k \pm \omega)(t_1 - t_2)} \\ & \rightarrow 2\pi f[(E_k - E_j)] \delta(t_1 - t_2) \theta(E_k - E_j). \end{aligned} \quad (\text{A8})$$

where neither the introduced infrared cut-off, ω_{min} nor the residual terms contribute to leading order, as defined above.

Using Eqs.(A6), (A7) and their counterparts for the two other orderings in Eq.(6), doing the t_2 integral (with the delta function symmetrically smeared, as can be justified by more accurate integrations) and differentiating with respect to t gives,

$$\begin{aligned}
\frac{d}{dt} \rho_I(E_j, t) &= \sum_{E_k} e^{i\lambda(E_j)t} \zeta e^{-i\lambda(E_k)t} \rho_I(E_k, t) \\
&\times e^{i\lambda(E_k)t} \zeta e^{-i\lambda(E_j)t} \Gamma(E_k, E_j) \\
&- \frac{1}{2} \left(e^{i\lambda(E_j)t} \zeta^2 e^{-i\lambda(E_j)t} \rho_I(E_j, t) \right. \\
&\left. + \rho_I(E_j, t) e^{i\lambda(E_j)t} \zeta^2 e^{-i\lambda(E_j)t} \right) \sum_{E_k} \Gamma(E_j, E_k).
\end{aligned} \tag{A9}$$

Using Eq.(A5) we now regain Eq.(4).